Chemical Engineering Journal Advances 23 (2025) 100784

Contents lists available at ScienceDirect

Chemical Engineering Journal Advances

journal homepage: www.sciencedirect.com/journal/chemical-engineering-journal-advances

Sustainable removal of aqueous naproxen using a ternary magneto-biochar-clay composite: Competition with carbamazepine and influence of dissolved organic matter

Aleksandër Peqini [a,b,*], Paul N. Diagboya [c], Ferdi Brahushi [b], Rolf-Alexander Düring [a]

[a] Institute of Soil Science and Soil Conservation, Research Centre for BioSystems, Land Use and Nutrition (iFZ), Justus Liebig University Giessen, Heinrich-Buff-Ring 26, 35392 Giessen, Germany
[b] Department of Environment and Natural Resources, Faculty of Agriculture and Environment, Agricultural University of Tirana, 1029 Tirana, Albania
[c] Environmental fate of chemicals and remediation (EnFaCRe) laboratory, Department of Environmental Management and Toxicology, University of Delta, PMB 2090 Agbor, Nigeria

ARTICLE INFO

Keywords:
Feldspar
Grape cluster stalk
Naproxen
Magnetite
Carbamazepine
Adsorption

ABSTRACT

Low-cost magneto-biochar-clay (MBC) composite adsorbent prepared by a combination of synthesized Fe_3O_4, biochar (from grape cluster stalk), and feldspar clay was tested for naproxen removal from simulated and real contaminated aqueous solutions. Preliminary sorption results for naproxen and other contaminants showed higher removal efficiency of the MBC than the pristine materials. Naproxen adsorption optimum solid-liquid ratio was at 0.5 g/L and the adsorption equilibrium was attained in 720 min on this composite, while the optimum adsorption was achieved at solution pH of 2.5. The process was endothermic and better described by the Sips adsorption isotherm model. Adsorptive pore filling, electrostatic and hydrophobic interactions between the composite surfaces and the naproxen species were the main mechanisms of naproxen uptake. In a competitive adsorption study with carbamazepine, the two compounds showed higher competition at lower solution pH values. With increase in dissolved organic matter concentration in water, naproxen and carbamazepine sorption reduced significantly. The composite retained high removal efficiency (≥99 %) after five consecutive adsorption cycles. Naproxen removal efficiency in real environmental water (river water) containing low naproxen concentration (50 μg/L) was quite high (≈ 93 %). Based on this study, the composite is sustainable, cost-efficient, and potentially applicable for naproxen and carbamazepine removal from surface waters.

1. Introduction

The ubiquitous presence of emerging contaminants, especially the pharmaceutically active compounds in surface water bodies is alarming; this is mostly so in low- to middle-income countries due to non-existent or poor wastewater treatment technologies [1]. Major input sources of pharmaceuticals include effluents from pharmaceutical plants, human and veterinary hospital effluents, excretion of semi/un-metabolized pharmaceuticals by humans and animals, as well as discharges from the municipal sewage system [2]. These compounds pose several risks to the ecosystem and human health because some of them have poor degradability and can bioaccumulate, this leads to longer exposure time in the environment which can result in drug resistant microbial species, and most have been reported to have adverse effects on non-target species [3].

Naproxen, a nonsteroidal anti-inflammatory drug (NSAID) is one of the frequently detected pharmaceuticals in the environment, particularly in surface waters with concentrations ranging from ng/L to μg/L [1, 4–7]. The frequent detection of naproxen in water may be related to its continuous discharge and low removal efficiency (<15 %) by conventional water treatment processes [8]. Naproxen is preferred in the treatment of osteoarthritis, rheumatoid arthritis, fever, and pain. Its widespread preference and use is attributed to several factors, including rapid absorption, long duration of action, high binding affinity to plasma proteins, lower vascular risk, and easy purchase without prescription [9]. Naproxen adverse effects to ecosystems and biota are mainly attributed to the toxicity of its metabolites including hydroperoxide, ketone, alcohol, etc. These metabolites (hydroperoxide, ketone) are

* Corresponding author at: Institute of Soil Science and Soil Conservation, Research Centre for BioSystems, Land Use and Nutrition (iFZ), Justus Liebig University Giessen, Heinrich-Buff-Ring 26, 35392 Giessen, Germany.
E-mail address: aleksander.peqini@umwelt.uni-giessen.de (A. Peqini).

https://doi.org/10.1016/j.ceja.2025.100784

Available online 3 June 2025

reported to have more toxicity than the parent compound to *Vibrio fischeri* and *Daphnia magna* [10]. Naproxen has adverse effects on gastrointestinal and renal activity of zebrafish and its embryos [8,11]. A concentration higher than 1 g/L has been reported to cause genotoxic effects in microorganisms such as *Bacillus thuringiensis* [12]. Carbamazepine, used in epileptic cases, also considered in this study is one of the most detected pharmaceuticals in water bodies [1]. Carbamazepine is another important and commonly used medication, and its photolytic metabolites are reportedly toxic to bacteria (*Vibrio fischeri*), algae (*Pseudokirchneriellasubcapitata*), and *Daphnia magna* [13]. The acute toxicity of this compound to fish, such as the Rainbow Trout (*Oncorhynchus mykiss*) makes it a very harmful compound for aquatic systems [14]. Therefore, it is of high importance to remove these compounds from water.

Pharmaceuticals could be removed from water *via* different techniques, including adsorption, physico-chemical/biological processes, or their combinations. The adsorption process has several advantages compared to the most techniques due to easy handling and operation, sustainability (when obtained from agro-organic waste), formation of zero-to-little harmful by-product, and cost-effectiveness. Several agro-organic wastes have been studied for naproxen removal from water, such as grape branches [15], rice straw [16], peanut shells [17], sheep manure [18], palm date and orange peel [19], bamboo [20], and wild plum kernels [3]. Major shortcomings of most natural adsorbents include bleeding of the adsorbents, low adsorption efficiencies, low durability/stability, and cumbersome post-adsorption separation of adsorbents from water. Thus the elimination of these flaws is the focus of most recent studies, and synergistic combination of two or more low-cost materials such as biomass, clays and magnetic nanoparticles have been proposed to overcome these [21–23]. It has been confirmed that biochar and clay combination increases the surface area, adsorption sites, improves the porosity, and adsorbent stability and reusability compared to the starting materials [24–27]. Irrespective of these attributes, post-adsorption (after adsorption process) separation of adsorbent from treated water remains a challenge. Recently, magnetization of adsorbents has been proposed and studied, and it has been found to make adsorbents easy to handle, the process simple to operate, and it saves cost [22,28]. Thus, the aim of the study was to prepare a low-cost adsorbent from agrowaste that can be magnetically separated from treated water post-adsorption.

In the current study, grape cluster stem bio-waste collected from a farm in Albania was used to prepare the composite. Due to favorable climatic conditions, grape cluster is a major agro-waste in Albania running into several thousand tons per year and thus sufficient quantity can be obtained for water treatment purposes. As a European Union candidate country, Albania has to align its water policy with the Water Framework Directive (Directive 2000/60/EC), which requires a good ecological and chemical status for all its water bodies. Albania is a middle-income country (World Bank, 2022), and has over 30 % of its population located in the central-western region, where the Ishmi river basin is located. Notably, this area lacks functional wastewater treatment plants, raising concerns about environmental pollution. Naproxen was selected for this study because it was detected almost in all collected water samples along the Ishmi river during a two-year study (2023-2024), with concentrations ranging from 0.3 μg/L to 2.6 μg/L, and an average concentration of 1 μg/L over the study period (our unpublished preliminary data). These findings align with the national data on naproxen consumption, where monthly average usage for the years 2022, 2023, and 2024 was reported at 119.3, 156.6, and 140.6 kg, respectively. Carbamazepine was also detected with concentrations ranging from 0.17 μg/L to 1.32 μg/L, and the monthly average usage for the years 2022, 2023, and 2024 was 45.6, 36, and 46 kg, respectively. It is important to note that these amounts reflect only the reimbursed quantities by the state (Mandatory Health Insurance Fund of Albania). The connection between the detected environmental concentrations of naproxen and carbamazepine, and their consumption underscores the potential negative impact on the aquatic environment. These results highlight the need for the establishment of effective wastewater treatment infrastructure in Albania to reduce pharmaceutical presence and protect water resources. Hence, the objective of this study was to prepare magneto-biochar-clay composite using grape cluster waste, feldspar clay, and magnetic nanoparticles for the removal of naproxen and carbamazepine from water.

2. Materials and methods

2.1. Materials, pretreatments, and ternary magnetic composite preparation and characterizations

Pretreated Feldspar clay (FLC) [29] and precleaned grape cluster stalk waste (GC) were the main low-cost materials used in this study. The GC was dried at 40 °C until a constant weight was achieved, then pulverized, sieved (1000 μm size sieve), and stored. Mettler Toledo scale (ME 204), MilliQ (Purelab, UK) water at 18.2 MΩcm, pH meter (inoLab® pH 7110), and HPLC grade acetonitrile (ACN) were used in this study. Naproxen, carbamazepine, sodium azide (NaN_3), formic acid, and humic acid sodium salt were purchased from Merck-Sigma-Aldrich GmbH, Germany. Ethanol and acetic acid were purchased from Carl Roth GmbH & Co. KG (Karlsruhe, Germany). The Strata C-18 cartridges were purchased from Phenomenex, USA.

The FLC and GC were employed alongside the synthesized magnetic nanoparticles (MNP) to prepare the ternary magneto biochar-clay composites (MBC-x). The average mass of raw GC which gave the specific mass of biochar (BC) was determined by calcination of triplicate (same) mass of GC for 2 h (in limited air) at a temperature of 500 °C. The MNP was prepared *via* chemical co-precipitation [30] by mixing $FeCl_3$ (7.8 g) and $FeSO_4{\cdot}7H_2O$ (3.9 g) in 400 mL water under continuous magnetic stirring. A solution of 2.0 M NaOH was added drop-wise until the red solution turned black. The MNP in the mixture was obtained by magnetic separation or centrifugation (5 min; 2500 rpm). It was washed (6x) with MilliQ water, dried at 40 °C, weighed, and stored in an air tight container.

Two ratio combinations of MBC-x (1:2:1 and 1:3:1) were prepared using the MNP, BC and FLC. The procedure started by preparing the MNP as described above but without the separation step. The calculated raw GC mass which gave the specific BC ratio was then added before shaking at 200 rpm for 30 min, and the subsequent addition of the FLC mass to give the specific ratio. The entire mixture was further agitated for 2 h, centrifuged at 1500 rpm for 10 min, and dried at 80 °C overnight before being calcined inside a crucible, as described above. The composites (MBC-1:2:1 and MBC-1:3:1) were cooled, washed till neutral, sieved, weighed, and stored.

The individual adsorbents and the composites were characterized for their cation exchange capacity (CEC) using the sodium saturation method and point of zero charge (pHpzc) using pH-drift method [31], as well as using the Fourier transform infrared (FTIR) spectrometer (VERTEX70, Bruker Optics, Germany) for the analysis of functional groups, the X-ray diffractometer (XRD) (Empyrean spectrometer, Malvern Panalytical, Germany) to assess crystallinity, the QUADRASORBevo analyzer (Quantachrome Instruments, USA) determining specific surface area, and the scanning electron microscope (SEM, Gemini SEM 560 Zeiss, Germany) in order to depict surface morphology.

2.2. Adsorption experiments

Standard stock solutions of naproxen and carbamazepine (10000 mg/L) were prepared in 50:50 ACN:MilliQ and stored at 4 °C, while the working solutions were prepared from the stock solution in MilliQ with 100 mg/L NaN_3, (biocide). To eliminate the co-solvent effect, the ACN amount in solution was kept at <0.1 %. Preliminary batch sorption experiments were carried out using 20 mg of either BC, FLC, MNP, or MBC (separately) in 10 mL of 1 mg/L of naproxen solution. Other

separate preliminary tests were performed using 20 mg mass in 15 mL of 2 mg/L terbuthylazine, 15 mL of 5mg/L Pb(II), and 30 mL of 5 mg/L Cu (II). Considering the ease of separation of the MBC 1:2:1 composite from water impacted by the magnetic property and its high adsorption performance compared to other tested materials, the MBC 1:2:1 composite was employed in the detailed batch adsorption study. Each batch experiment used 5 mg mass (except for mass effect study) of adsorbent in 10 mL of 2.5 mg/L naproxen solution (except for concentration effect study) at pH of 4.5 ± 0.1 (except for the study of pH effect) using 20 mL brown glass vials incubated for 1440 min (except for kinetics study) at 200 rpm and 20 °C (except for temperature effect study). The solution pH adjustment was carried out using 0.2 M HCl or NaOH. The effects of several adsorption parameters such as adsorbent mass from 5-40 mg, time from 1-1440 min, solution pH from 2.5-10, naproxen concentration from 1-20 mg/L, and ambient temperature from 20-40 °C were investigated. Naproxen desorption was performed after equilibrium at 20 °C in order to get more insight to the adsorption mechanism. The desorption process was carried out using the composite that was magnetically separated from the naproxen solution, dried overnight at 40 °C, and the vials with the same residual composites were refilled with the same background solution/biocide (without naproxen). The competition with carbamazepine was assessed with 5 mg adsorbent mass, at varying solution pH (2.5-10) and 2.5 mg/L concentration for both compounds. The effect of dissolved organic matter (DOM) with humic acid sodium salt (5-100 mg/L) and a concentration of 2.5 mg/L each naproxen and carbamazepine, using 5 mg adsorbent at a solution pH of 4.5 ± 0.1, was evaluated. The sorption with pristine river water (pH 4.5 ± 0.1) with 2.5 mg/L naproxen and carbamazepine, and 5 mg adsorbent mass was also evaluated. The composite's reusability was assessed using 5 mg of the used-adsorbent and naproxen solution concentration of 2.5 mg/L. The adsorbed naproxen was desorbed by shaking in 10 mL of ethanol twice (200 rpm for 1 h) and rinsed in MilliQ water under the same conditions, before drying overnight and reusing. Five cycles of reusability were carried out. The composite's applicability and removal efficiency was evaluated in river water (collected from the Ismi river in Albania), which was spiked with similar environmental naproxen concentrations (50 μg/L). For the naproxen determination in this last experiment, samples were concentrated by using C-18 Strata cartridges and extracted with 2 mL ACN:acetic acid (80:20, v:v). After each experiment, the solutions were filtered with 1 μm glass fiber filters, and analyte concentration remaining in solution was measured using HPLC-DAD.

2.3. Naproxen and carbamazepine determination

A previously reported analytical method for the determination of naproxen and carbamazepine determination [32] was applied. Naproxen and carbamazepine were analyzed by an Agilent 1200 HPLC system (Agilent Technologies Inc., USA), equipped with a reverse-phase, C18 column (3 μm, 120 Å, 2.1 × 150 mm), column oven, autosampler, quarternary pump, and a DAD detector . The device was operated at 35 °C with an injection volume of 20 μL. The mobile phase consisted of a mixture of acetonitrile:0.2 % formic acid in water (60:40, v:v) at a flow rate of 0.3 mL/min. The wavelengths of 230 nm and 285 nm, and 8 min run time (3.38 and 2.1 min retention time) were employed for naproxen and carbamazepine, respectively. The naproxen and carbamazepine calibration curves exhibited a linear range with r^2 of 1 using concentrations between 0.05 and 20 mg/L, and 0.5 – 20 mg/L in 100 mg/L biocide (NaN_3) for naproxen and carbamazepine, respectively. Using blanks, naproxen and carbamazepine sorption on the vials walls, caps, and filters were found to be negligible.

2.4. Data treatment and adsorption model fittings

The amounts (mg/g) of naproxen and carbamazepine adsorbed (q_e) were calculated from Eq. 1 (SM Table 2). Kinetics of naproxen sorption was evaluated using the nonlinear forms of the pseudo-first-order (PFO) (SM Table 2 Eq. 2), pseudo-second-order (PSO) [33] (SM Table 2 Eq. 3), and the intra-particle diffusion (IPD) [34] (SM Table 2 Eq. 4) models. The Langmuir (SM Table 2 Eq. 5), Freundlich (SM Table 2 Eq. 6), and the Sips non-linear adsorption isotherm (SM Table 2 Eq. 7) models were fitted to the equilibrium adsorption data and used to describe the naproxen uptake process. The dimensionless equilibrium constant K^0 (L/g) was calculated from Eq. 8 (SM Table 2), while the thermodynamic parameters were determined from Eq. 9 and 10 (SM Table 2) using equilibrium adsorption data at 293.15, 303.15, and 313.15 K. The model fittings and models' parameters were obtained using the OriginPro 2015 software (OriginLab Corporation, USA). All equations and parameters are shown in SM Table 2.

3. Results and discussions

3.1. Characterization of adsorbents

The characterization results of the starting materials adsorbents and composites are presented in Figs. 1 and 2 and SM Table 1. The pHpzc was first determined because an adsorbent's pHpzc is an important property that determines its surface charge state at varying solution pH (SM Fig. 1). The surface charge density is positive below the pHpzc, thus, the adsorbent attract negatively charged ions, while above the pHpzc, the charge is negative and the surface attracts positive ions. The pHpzc (SM Table 1) of the BC was quite alkaline (pHpzc of 10.0) unlike those of the MNP and FLC which were near neutral and slightly acidic, respectively. The MBC composites exhibited similarly high pHpzc values (mean value of 9.3) as the BC, and this suggests that the BC component of the composite has a particularly strong effect on its property. The alkaline pHpzc values are in agreement with reported values for other biochar composites [30,35]. Evaluation of the cation exchange capacity (CEC) values (SM Table 1) of the composites indicated average percentage decreases of ≈48 and 16 %, respectively, in comparison to the BC and MNP values, but these values were significantly higher than the FLC value. The BET specific surface area values (SM Table 1 and Fig. 1d) of the composites were not substantially different from the BC values but significantly lower than that of the MNP, thus highlighting the dominant contribution of the BC in the composite.

The FTIR spectra (Fig. 1b) scanned between 4000 and 500 cm^{-1} for the precursor adsorbents and the composites showed that the major functional groups associated with the precursor adsorbents were transferred to the composites. For instance, the FLC and BC peaks around 1035 cm^{-1} attributed to Si-O in-plane bending vibrations, as well as the FLC peaks at 730 and 525 cm^{-1} ascribed to Si-O-Si bridging bonds in SiO_2 and Al-OH/Al-O deformations, respectively [30], were observed in the composites although with slight shifts. The signature Fe_3O_4 MNP Fe-O peak at ≈560 cm^{-1} was also noticeably transferred to the composites; indicating the presence of magnetic property in the composites [36]. The composites' peaks between 1585 and 1420 cm^{-1} are characteristic of C=O, C=C aromatic stretching rings, and amide-I groups, while those at ≈3200 cm^{-1} for all adsorbents were attributed to –OH groups possibly from water [34,37,38].

Evaluation of the crystallinity using the XRD (Fig. 1c) expressed the presence of the signature FLC peaks ascribed to microcline, quartz, and feldspar minerals at 2θ of 22.0, 26.6, 27.9°, respectively, as well as the partial triclinic feldspar mineral peak at 30.7°. Typical Fe_3O_4 spinal structures were present at 2θ of 30.3, 35.5, 43.1, 57.1, and 62.7. Similar to the FTIR spectra, these unique XRD peaks of the FLC and MNP were transferred to the composites, an indication that there were no significant lattice changes in the primary components of the composites [28, 30]. The morphological structure of these adsorbents observed *via* the SEM (Fig. 2a–f) showed that the composites (Fig. 2e-f) were truly a combination of materials by exhibiting the honey comb porous nature of the BC (Fig. 2b) as well as the spinal MNP (Fig. 2d), thus, confirming a successful composite preparation.

Preliminary naproxen sorption experiments, conducted to evaluate

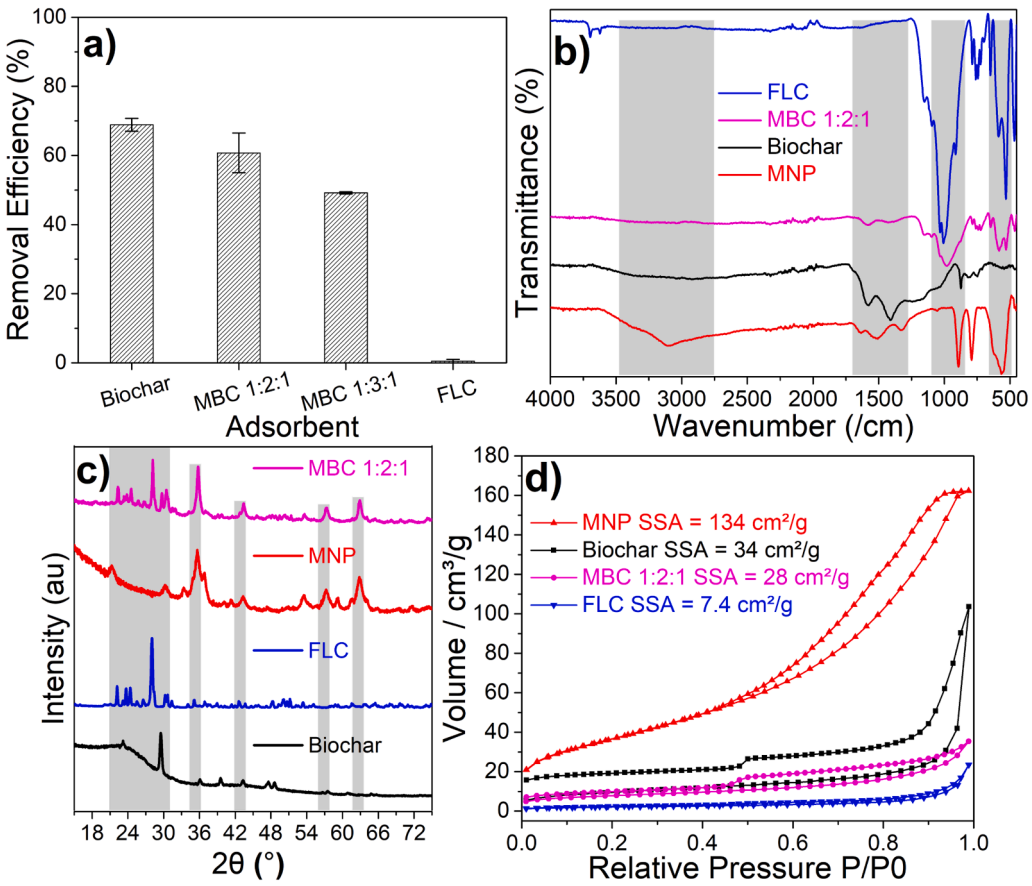

Fig. 1. (a) Preliminary experiment showing naproxen removal efficiencies of the starting materials and composite; (b) comparative FT-IR spectra peaks of the starting materials and composite; (c) XRD diffractograms of the starting materials and composite; and (d) nitrogen adsorption/desorption isotherms (showing the BET specific surface areas).

and compare the sorption potentials of the starting materials and composites showed highest removal efficiency in the BC with 68.8 % removal, followed by MBC 1:2:1 and MBC 1:3:1 with 60.7 % and 49.1 %, respectively (Fig. 1*a*). FLC exhibited very low removal efficiency (<0.5 %). Due to the lack of magnetic properties in the BC, the MBC 1:2:1 was selected as the best performing adsorbent to be used for determining the optimized sorption parameters. Further preliminary sorption tests using two inorganic contaminants (Cu(II) and Pb(II)) and another organic contaminant (terbuthylazine) (SM Fig. 2) showed that the MBC 1:2:1 composite exhibited the highest removal efficiency compared to other adsorbents with ≈95.7, 99.7, and 76.6 % for Cu(II), Pb(II), and terbuthylazine, respectively.

3.2. *Mass optimization, sorption kinetics, and effect of pH*

The adsorbent dosage directly impacts the amount of contaminant adsorbed due to changing availability and access to adsorption sites as more or less particles interact with the contaminants in solution [39]. Thus, the composite's adsorbent dosage optimization was carried out in a mass range of 5-40 mg in 10 mL (0.5-4 g/L) of 1 mg/L naproxen solution at 1440 min incubation (Fig. 3a). It was observed that with increasing adsorbent dose, the amount of naproxen adsorbed was decreased from 1.71 mg/g to 0.20 mg/g. The removal efficiency also exhibited similar trend, gradually decreasing from 90 % to 85 % with increase in mass. This diminution in the percentage naproxen adsorbed at higher adsorbent loading may be ascribed to an increased aggregation of the adsorbents which resulted in the subsequent unavailability of adsorption sites and reduced adsorption [16]. Based on the obtained data, 5 mg (0.5 g/L) of the adsorbent was selected as the optimum mass for naproxen adsorption.

The sorption rate trend of naproxen on the MBC 1:2:1 composite was carried out using 5 mg adsorbent in 10 mL of 2.5 mg/L naproxen solution. The results, depicted in SM Fig. 4a, showed a fast naproxen uptake from the composite in the first 180 min, which corresponds to naproxen uptake on the richly available vacant adsorption sites as well as its diffusion from the solution phase to the pores at the beginning of the process [22]. Thereafter, the adsorption process was gradual until equilibrium which was reached at about 720 min. The uptake process here was mainly characterized by the slow diffusion of naproxen into the micropores [40,41]. Subsequent experiments were carried out over 1440 min because at this time, a stable equilibrium was well established.

Three adsorption kinetics models (PFO, PSO, and IPD) were employed in evaluating the naproxen uptake process and their fitting curves and estimated models' parameters are presented in SM Fig. 4a and Table 1, respectively. The PSO model exhibited a higher correlation coefficient (r^2) and smaller chi-square (χ^2) values, with better correlated calculated q_e value than the PFO model. These values imply that the PSO model fit better to the rate data and indicate that the adsorption process was mainly controlled by sharing or exchange of valence electrons which resulted in attractive interactions including electrostatic and hydrophobic interactions between the adsorbent surfaces and the naproxen species [21,42]. In addition, an evaluation of the IPD model C (mg/g) parameter, which is a measure of the estimated surface concentration of the contaminant, indicated that less than 15 % of total adsorption occurred on the composite's surface; the bulk of the naproxen uptake were within the pores [43,44]. The multi-linear IPD plot (SM Fig. 4a) indicates that more than one stage is involved in naproxen adsorption: surface adsorption, and within the pores of the composite.

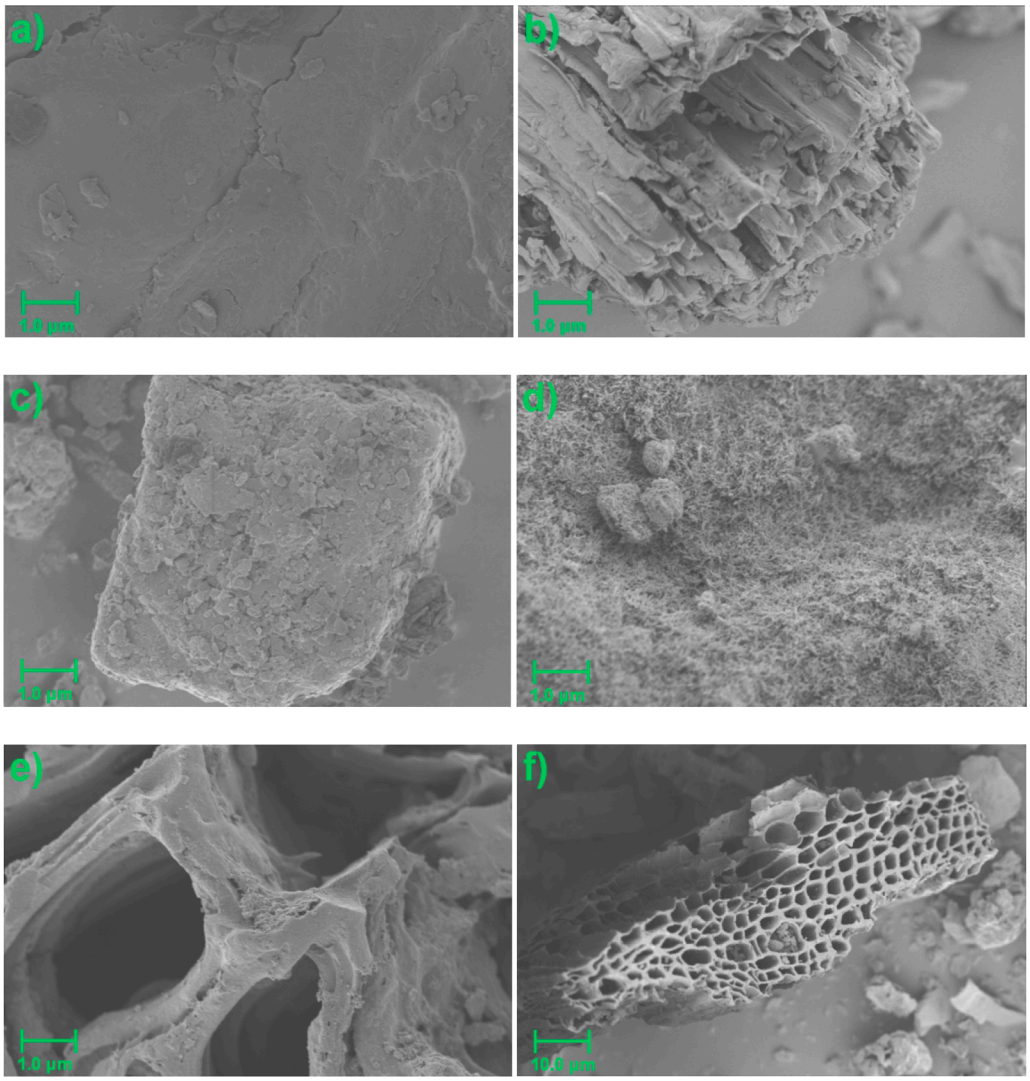

Fig. 2. SEM electron micrographs of (a) biomass; (b) biochar; (c) feldspar; (d) magnetic nanoparticles; (e) MBC 1:2:1; and (f) MBC 1:3:1.

Table 1
Kinetic model parameters for naproxen adsorption on MBC 1:2:1.

Kinetic model	Parameter	Naproxen MBC 1:2:1
PFO	q_e (mg g^{-1})	2.427
	k_1 (min^{-1})	0.008
	r^2	0.87
	χ^2	0.11
PSO	q_e (mg g^{-1})	2.768
	k_2 (g mg^{-1} min^{-1})	0.004
	r^2	0.93
	χ^2	0.058
IPD	C (mg g^{-1})	0.433
	k_i (g g^{-1} $min^{1/2}$)	0.073
	r^2	0.948
	χ^2	0.043
Experimental	mg/g	2.889

Naproxen is at first adsorbed through surface functional groups until saturation, and then diffused in the composite's porous sites [3].

Solution pH is recognized as a major interfering factor in contaminants uptake because it affects the degree of speciation of the contaminant as well as the adsorbent sites charge [35]. Hence, taking into account the physico-chemical properties of the naproxen molecule (SM Table-3), the effect of solution pH on the naproxen uptake by the MBC 1:2:1 composite was tested over five different solution pH (2.5, 4.5, 6.5, 8, and 10), and the adsorption trend is depicted in Fig. 3b. Naproxen has a dissociation constant (*pKa*) of 4.2 [45], and may be anionic or neutral depending on the deprotonation (H^+) of the carboxylic group [46]. Thus, at low solution pH, the neutral form predominates due to negligible deprotonation of the carboxylic group of the naproxen molecule, and uptake process is *via* hydrophobic interaction between the composite surface and aromatic rings of naproxen molecule, as well as through hydrogen bonds between the carboxylic group and composite's functional groups [46]; this is the reason for the higher uptake recorded at lower pH values. At pH 4.5, the adsorption is mainly *via* electrostatic interaction between the positively charged composite surface and anionic naproxen (pHpzc = 9.2) [17,20]. However, as pH increases, the composite's surface becomes progressively deprotonated and less positive, naproxen becomes increasingly anionic resulting in increased water solubility, weaker and fewer electrostatic interactions (electrostatic repulsion), and lower naproxen uptake. It is assumed that the naproxen uptake did not reduce to zero due to uptake or trapping of the naproxen molecules within the composite's pores.

3.3. Equilibrium adsorption at varying temperatures and adsorption isotherm modeling

Equilibrium adsorption of naproxen on MBC 1:2:1 composite at varying concentrations (1–20 mg/L), and temperatures (20, 30, and 40

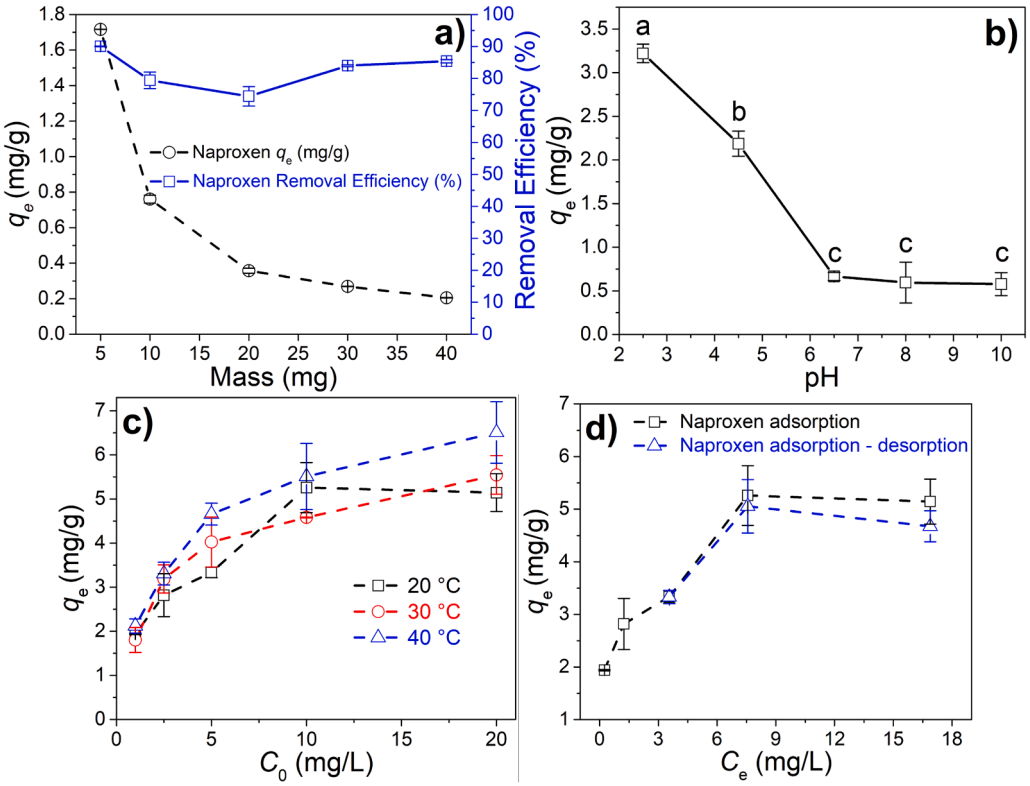

Fig. 3. (a) Adsorption trend and removal efficiency at varying MBC 1:2:1 dosage; (b) adsorption trend at varying naproxen solution pH; (c) effect of concentration and temperature on naproxen uptake; and (d) naproxen desorption at 20 °C.

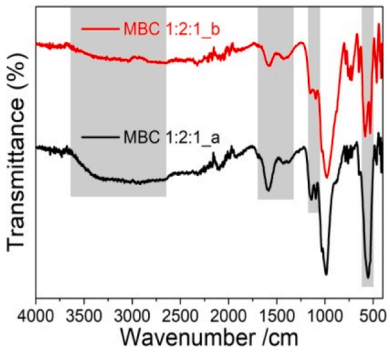

Fig. 4. Comparison of pre-adsorption (before adsorption process, MBC 1:2:1_b) and post-adsorption (after adsorption process, MBC 1:2:1_a) FTIR spectra.

°C), was studied and the trends in mg/g and percentages are given in Fig. 3c and SM Fig. 3, respectively. The trends showed increasing amounts of naproxen sorption as the concentration increased until equilibrium was attained at 10 mg/L concentration (Fig. 3c). Similar trends have been reported in the literature [16,46]. This increased uptake at higher concentration may be attributed to two sorption phenomena: multi-layer adsorption resulting from by π-π interactions and the behavior of naproxen molecules as concentration increased [27,31]. On one hand, due to the presence of electron-deficient π-bonds on the benzene ring structures of the naproxen molecule, it is possible for π-π interaction to occur between adsorbed naproxen and another naproxen molecule in solution leading to multi-layer adsorption at higher concentrations [31]. In addition, at higher concentrations, the potential for the transfer of naproxen molecules from the saturated composite's external surfaces to the inner pore surfaces becomes higher leading to the observed enhanced adsorption [27]. Evaluating the equilibrium data in terms of efficiency of naproxen uptake showed a decreasing efficiency trend as concentration increased (SM Fig. 3), and this may be ascribed to the limited active adsorption sites at fixed composite mass, thus, relative to the increasing concentration of naproxen, the efficiency will be progressively lower.

Evaluating the effect of ambient temperature on naproxen uptake showed a slightly increased uptake with higher temperature (Fig. 3c). Similar trend has been reported by other authors studying biochar based adsorbents [46,47], and this trend was attributed to the energy input into the system at higher temperature which was helpful in breaking the repulsive force (activation energy) hindering naproxen adsorption. The increase in adsorption at higher temperatures might be due to the increment of naproxen mobility (which enhances further migration into the adsorbent pores), as a result of breaking hydrogen bonds (water – COOH), and solute hydrophobicity (which may favor the hydrophobic interactions between naproxen and the composite) [46]. In addition, at high temperatures, the porosity and pore volume may have been increased, thus improving naproxen uptake [16]. This naproxen uptake trend suggested that the process was endothermic, thus the data was evaluated to obtain the thermodynamic variables (Table 2) and describe the process appropriately. The positive ΔH confirmed that the process was endothermic, thus an increase in temperature would result in an increase in naproxen uptake. The negative ΔG and its increasing magnitude with temperature indicate that the adsorption process is spontaneous and becomes more favorable at high temperatures, while the ΔS (> 0) suggested an increased randomness (mobility) of the naproxen molecules on the composite's external surface at equilibrium [18].

Further evaluation of the naproxen equilibrium adsorption data were obtained by fitting three adsorption isotherm models (Langmuir, Freundlich, and Sips) to the data as depicted in SM Fig. 4b-d with the model parameters shown in Table 2. Analysis of the fitting parameters, r^2 and χ^2, showed that the Sips model described the equilibrium data better than the Freundlich and Langmuir models. This suggests that naproxen uptake process comprised of complex interactions occurring

Table 2
Naproxen adsorption isotherm model parameters and calculated thermodynamics parameters for naproxen uptake.

Adsorption isotherm model	Parameter	293.15 K 20 °C	303.15 K 30 °C	313.15 K 40 °C
Langmuir	Q_o (mg/g)	5.241	5.309	6.185
	β	1.135	1.396	1.524
	r^2	0.721	0.93	0.812
	χ^2	0.594	0.14	0.567
Freundlich	$1/n$	0.245	0.236	0.233
	K_F	2.734	2.88	3.444
	r^2	0.866	0.95	0.99
	χ^2	0.285	0.099	0.03
Sips	q_{max} (mg/g)	6.726	6.148	8.516
	$1/n$	0.305	0.35	0.265
	K_S (L/mg)	0.053	0.131	0.034
	r^2	0.82	0.951	0.991
	χ^2	0.381	0.098	0.025
	ΔG° (kJ/mol)	-17.14	-18.25	-19.08
Thermodynamics	ΔH°(kJ/mol)	11.29	11.29	11.29
	ΔS° (J/mol/K)	97.1	97.1	97.1

on heterogeneous composite surfaces of unequal affinity for the naproxen molecule in solution [27]. Some of these interactions have been suggested above and include electrostatic interactions, π-π interactions leading to multi-layer adsorption, as well as possible hydrogen bonding, and pore filling or entrapment within the composite pores.

3.4. Adsorption mechanisms

Considering the FTIR spectra results, the composite properties, speciation of naproxen, and adsorption trends, possible mechanisms of naproxen adsorption onto the composite were proposed (Fig. 5). An examination of the naproxen post-adsorption effect (after adsorption process) on the FTIR spectra (Fig. 4) showed that the broad peak around 3200 /cm which was attributed to the –OH groups exhibited the highest change in intensity after the adsorption process (region 3600 – 2600 /cm), indicating that the –OH groups of the composite were the main contributors to the naproxen adsorption process *via* electrostatic interactions and H-bonding; the composite's adsorption site acts as the H-donor while the deprotonated naproxen molecules is the H-acceptor. Similar FTIR trend has been reported [3] for naproxen adsorption on biochar. Taking into account that the adsorption conditions were at solution pH 4.5 and the composite's pHpzc of 9.2, these interactions occur due to the positive charge of the composite and the negatively charged naproxen ions. Furthermore, the FTIR spectra showed that the aromatic stretching vibrations corresponding to the C=O and C=C groups (peaks between 1585 and 1420 /cm) showed higher intensities. This response of the C=C bond indicates the presence of π-π interactions between the benzene rings of naproxen with the graphitic planes of the carbonaceous structure of the composite [48]. On the other hand, that of C=O groups, suggests n-π interactions between the oxygen electron pairs (n-electron donors) of hydroxyl groups of naproxen with composite's electron-depleted sites [3,40]. Another peak that showed enhanced vibration after the adsorption was the magnetic Fe–O (≈ 560 /cm), indicating an interaction of $–COO^-$ of naproxen molecules with Fe–OH impregnated on the MBC 1:2:1 composite surface [28]. Also, the desorption of adsorbed naproxen on MBC 1:2:1 composite at 20 °C using the same background electrolyte/biocide solution (Fig. 3d) showed a low desorption especially at low naproxen adsorption concentrations (<3 mg/L). This data suggests a high entrapment of naproxen on the pores of the composite, thus, supporting and confirming the IPD model *C* (mg/g) parameter, which showed that the bulk of the naproxen uptake process occurred within the composite's pores.

3.5. Competitive sorption of naproxen and carbamazepine and effect of dissolved organic matter

The effect of solution pH on naproxen and carbamazepine uptake from single and binary solutions was tested under the same conditions (as described in section 3.2), and the adsorption trends are given in Fig. 6*a*. Carbamazepine has two dissociation constants (*pKa*) values of 2.3 (ketone group) and 13.9 for the $–CONH_2$ (amine) group [49]. Thus, at all tested solution pH values, it existed as neutral compound. Under these conditions, carbamazepine adsorption onto the composite mostly involved hydrophobic, π–π interactions and hydrogen bonding [50]. In addition, the post FTIR spectra of composite after single carbamazepine sorption, showed same region response as post-naproxen-sorption spectra, indicating that same sites were responsible for their adsorption (SM Fig. 5). Due to the positive charge of the composite (pH <pHpzc), cation-π interactions may occur with the π-system (benzene ring) of carbamazepine [51]. From the adsorption trends in the binary system, it was observed that at the solution pH <4.5, both compounds had high sorption though naproxen sorption was higher. This sorption trend could result from strong hydrophobic interactions and the highly porous and heterogeneous nature of the composite [3]. Interestingly, with increasing solution pH the sorption of carbamazepine surpasses that of naproxen both in single and binary solution though the amounts

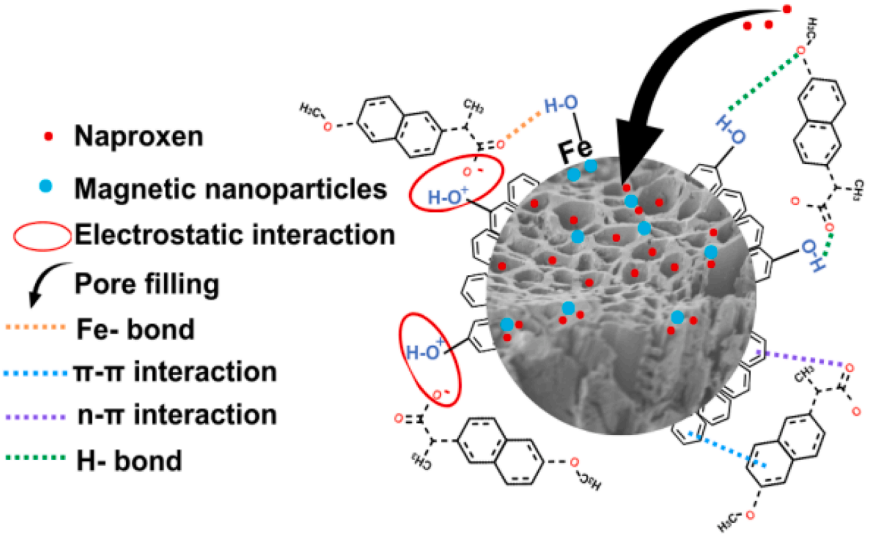

Fig. 5. Proposed adsorption mechanisms of naproxen onto MBC 1:2:1 composite in a SEM electron micrograph (magnification: 10 μm).

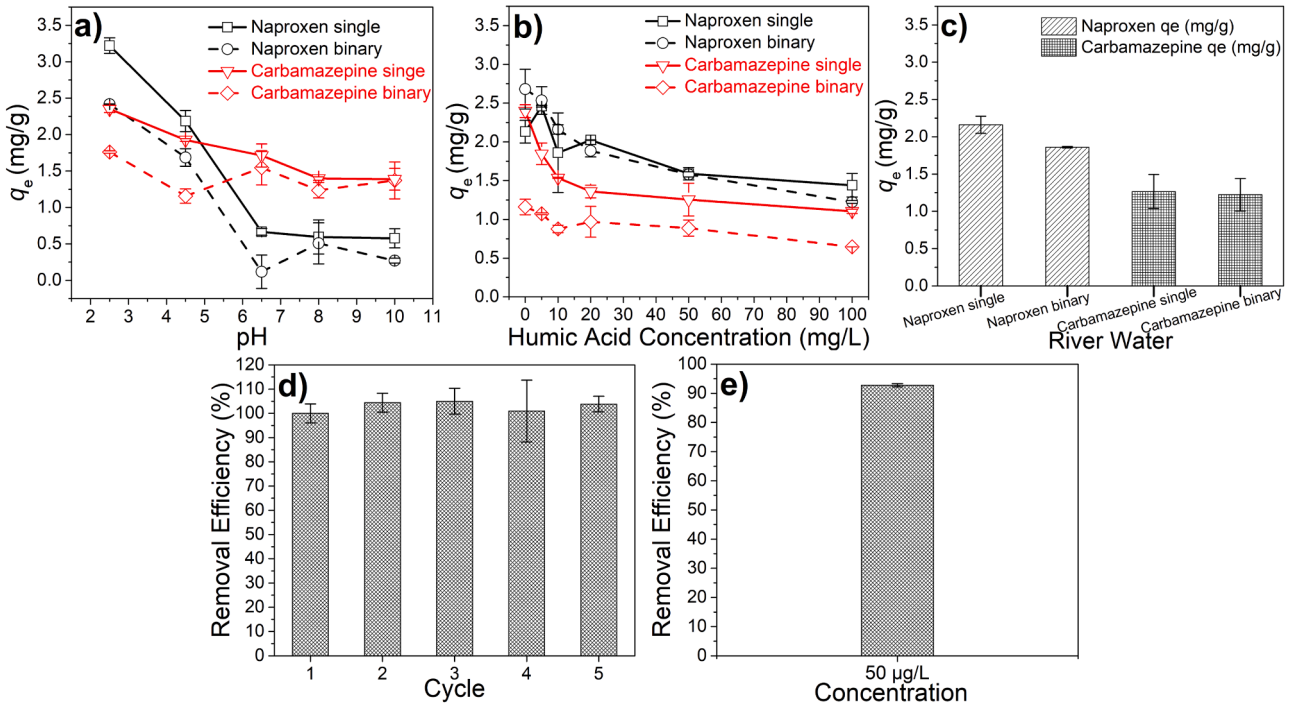

Fig. 6. (a) Competitive adsorption of naproxen and carbamazepine, (b) effect of dissolved organic matter on naproxen and carbamazepine sorption, and (c) adsorption of naproxen and carbamazepine in river water; (d) comparative reusability of naproxen over 5-cycles, and (e) removal efficiency with Ishmi river water at 50 µg/L *naproxen concentration*.

adsorbed were lower than at low pH. This trend suggests strong competition between naproxen and carbamazepine at lower pH but at the higher pH range the competition was weak and carbamazepine sorption exceeded naproxen.

The presence of DOM in wastewater effluents directly impacts and is considered as the main limiting factor in organic compounds sorption [52]. Therefore, the effect of DOM on naproxen and carbamazepine sorption onto the composite was tested over five different humic acid concentrations (5-100 mg/L), while the concentrations of naproxen and carbamazepine remained fixed at 2.5 mg/L. The sorption trends depicted in Fig. 6*b* showed that at very low DOM concentration (5 mg/L), the uptake of naproxen in single solution slightly improved from 2.13 to 2.46 mg/g. After this, a gradual naproxen sorption decrease was observed, reaching 1.44 mg/g at 100 mg/L DOM concentration. Similarly, in binary system, naproxen showed a similar decreasing trend. This trend may be related to the discussion above; the pHpzc of the composite had a value of 9.2, and at solution pH of 4.5, the composite net charge is positive and naproxen exists as a deprotonated molecule, indicating a significant electrostatic interaction. Also at the same pH conditions (pH 4.5), humic acid substances are negatively charged, thus as humic acid adsorb onto the composite surface, the adsorption of naproxen (mainly negatively charged) would decrease due to repulsion forces [53]. Carbamazepine in the single system showed an immediate decrease in sorption with increasing humic acid concentration from 5-20 mg/L, with initial decrease of 1.84 and 1.36 mg/g, respectively. After this, a slight decrease was observed, reaching 1.1 mg/g at 100 mg/L humic acid concentration. The relatively high presence of oxygen containing functional groups such as –COOH, –OH, and C=O in humic acid, could result in complex formation with biochar and probably with carbamazepine, indicating a high competition between these groups and carbamazepine for the composite's active adsorption sites and hydrophobic interactions, thus decreasing the amount of adsorbed carbamazepine on the composite [54,55]. Meanwhile, carbamazepine sorption in binary system (with naproxen) was lower compared to that of single system, indicating a higher competition. The composite sorption potential for naproxen and carbamazepine at 2.5 mg/L concentrations, 5 mg mass, and solution pH of 4.5 in single and binary systems was tested in river water, and the results are given in Fig. 6*c*. The composite showed similar sorption capacities as 20 mg/L DOM concentration (total organic carbon of river water = 25.7 mg/L), with 2.16 and 1.85 mg/g for single and binary systems for naproxen, and 1.26 and 1.22 mg/g for single and binary systems for carbamazepine, respectively.

3.6. *Reusability*

The reusability of the MBC 1:2:1 was investigated in five adsorption cycles and the results are presented in Fig. 6*d*. In addition, the naproxen uptake by the composite using environmentally relevant concentration was also tested with Ishmi river (Albania) water (spiked with 50 µg/L) and the results are given in Fig. 6e. The removal efficiency for naproxen in the first cycle was adjudged to be 100 %. After that, during the four subsequent cycles, the removal efficiency remained around ≈100 % (compared to the first cycle), thus, no significant difference was observed. Interestingly, the results with Ishmi river water, using environmentally relevant naproxen concentration showed a removal efficiency of ≈92.8 %. Therefore, these results confirm that MBC 1:2:1 composite is potentially applicable and useful for naproxen and carbamazepine removal from water.

4. Conclusions

The adsorption of the pharmaceutical compound- naproxen was investigated onto a ternary magneto-biochar-clay composite (MBC 1:2:1), made from a combination of grape cluster biomass, feldspar clay, and Fe_3O_4. Characterization data indicated that the composite physicochemical properties such as pHpzc, CEC, BET surface area, morphology, and the functional groups presence were mainly impacted by biochar presence. Naproxen adsorption process was endothermic, and better described by Sips adsorption isotherm model. Adsorptive pore filling, electrostatic and hydrophobic interactions between the composite surfaces and the naproxen species were the main mechanisms of naproxen

uptake. The composite exhibited very good removal efficiency after five consecutive adsorption cycles as well as in real environmental water (river water) containing low naproxen concentration. Therefore, the prepared composite is sustainable, cost-efficient, and potentially applicable for naproxen removal from natural waters.

Competing interests

The authors have no relevant financial or non-financial interests to disclose.

Funding

This research did not receive any specific grant from funding agencies in the public, commercial, or not-for-profit sectors.

CRediT authorship contribution statement

Aleksandër Peqini: Writing – review & editing, Writing – original draft, Visualization, Validation, Software, Methodology, Investigation, Formal analysis, Conceptualization. **Paul N. Diagboya:** Writing – review & editing, Writing – original draft, Validation, Software, Project administration, Methodology, Formal analysis. **Ferdi Brahushi:** Writing – review & editing, Supervision, Project administration, Methodology, Funding acquisition, Conceptualization. **Rolf-Alexander Düring:** Writing – review & editing, Supervision, Resources, Project administration, Methodology, Funding acquisition, Conceptualization.

Declaration of competing interest

The authors declare that they have no known competing financial interests or personal relationships that could have appeared to influence the work reported in this paper.

Acknowledgements

We acknowledge the support of Deutsche Bundesstiftung Umwelt (DBU), Germany and the Erasmus+ program, for the support of the research fellowships to A Peqini, and the support of the Alexander von Humboldt Foundation, Germany, for the award of Georg Forster experienced research fellowship to PN Diagboya. Also, we acknowledge the support of the Department of Chemistry at JLU Giessen for technical assistance with the composite characterization.

Supplementary materials

Supplementary material associated with this article can be found, in the online version, at doi:10.1016/j.ceja.2025.100784.

Data availability

Data will be made available on request.

References

[1] J.L. Wilkinson, et al., Pharmaceutical pollution of the world's rivers, Proc. Natl. Acad. Sci. U S A (8) (2022) 119.
[2] K. Kümmerer, The presence of pharmaceuticals in the environment due to human use–present knowledge and future challenges, J. Environ. Manage. 90 (8) (2009) 2354–2366.
[3] O. Paunovic, et al., Ionisable emerging pharmaceutical adsorption onto microwave functionalised biochar derived from novel lignocellulosic waste biomass, J. Colloid Interface Sci. 547 (2019) 350–360.
[4] B.F. Da Silva, et al., Occurrence and distribution of pharmaceuticals in surface water, suspended solids and sediments of the Ebro river basin, Spain, Chemosphere 85 (8) (2011) 1331–1339.
[5] M. Petrovic, et al., Determination of 81 pharmaceutical drugs by high performance liquid chromatography coupled to mass spectrometry with hybrid triple quadrupole-linear ion trap in different types of water in Serbia, Sci. Total Environ. 468-469 (2014) 415–428.
[6] A. Lolic, et al., Assessment of non-steroidal anti-inflammatory and analgesic pharmaceuticals in seawaters of North of Portugal: occurrence and environmental risk, Sci. Total Environ. 508 (2015) 240–250.
[7] M. Papageorgiou, C. Kosma, D. Lambropoulou, Seasonal occurrence, removal, mass loading and environmental risk assessment of 55 pharmaceuticals and personal care products in a municipal wastewater treatment plant in Central Greece, Sci. Total Environ. 543 (Pt A) (2016) 547–569.
[8] T. Ding, et al., Biodegradation of naproxen by freshwater algae Cymbella sp. and Scenedesmus quadricauda and the comparative toxicity, Bioresour. Technol. 238 (2017) 164–173.
[9] D. Wojcieszynska, U. Guzik, Naproxen in the environment: its occurrence, toxicity to nontarget organisms and biodegradation, Appl. Microbiol. Biotechnol. 104 (5) (2020) 1849–1857.
[10] M. Della Greca, et al., Phototransformation and ecotoxicity of the drug Naproxen-Na, Environ. Chem. Lett. 1 (4) (2003) 237–241.
[11] Q. Li, et al., Acute toxicity and histopathological effects of naproxen in zebrafish (Danio rerio) early life stages, Environ. Sci. Pollut. Res. Int 23 (18) (2016) 18832–18841.
[12] D. Gorny, et al., Naproxen ecotoxicity and biodegradation by Bacillus thuringiensis B1(2015b) strain, Ecotoxicol. Environ. Saf 167 (2019) 505–512.
[13] E. Donner, et al., Ecotoxicity of carbamazepine and its UV photolysis transformation products, Sci. Total. Environ. 443 (2013) 870–876.
[14] Z.H. Li, et al., Acute toxicity of carbamazepine to juvenile rainbow trout (Oncorhynchus mykiss): effects on antioxidant responses, hematological parameters and hepatic EROD, Ecotoxicol. Environ. Saf 74 (3) (2011) 319–327.
[15] J. Georgin, et al., Woody residues of the grape production chain as an alternative precursor of high porous activated carbon with remarkable performance for naproxen uptake from water, Environ. Sci. Pollut. Res. Int 29 (12) (2022) 16988–17000.
[16] S. Bhattacharya, et al., Thermal, Chemical and ultrasonic assisted synthesis of carbonized Biochar and its application for reducing Naproxen: Batch and Fixed bed study and subsequent optimization with response surface methodology (RSM) and artificial neural network (ANN), Surf. Interfaces 26 (2021) 101378.
[17] F. Tomul, et al., Peanut shells-derived biochars prepared from different carbonization processes: Comparison of characterization and mechanism of naproxen adsorption in water, Sci. Total Environ. 726 (2020) 137828.
[18] M. Fatih Dilekoglu, M. Yapici, Adsorption of naproxen pharmaceutical micropollutant from aqueous solutions on superior activated carbon synthesized from sheep manure: Kinetics, thermodynamics, and mechanism, J. Mol. Liq. 381 (2023) 121839.
[19] Z. Dashti, et al., Effects of lignin on biochar from pyrolysis: emphasis on removing naproxen as pharmaceutical pollutants in wastewater, Clean Technol. Environ. Policy (2024).
[20] T.D. Pham, et al., Adsorption characteristics of ciprofloxacin and naproxen from aqueous solution using bamboo biochar, Biomass Convers. Biorefinery 15 (2) (2023) 3071–3082.
[21] Z. İlbay, et al., Isolation of naproxen from wastewater using carbon-based magnetic adsorbents, Int. J. Environ. Sci. Technol. 12 (11) (2015) 3541–3550.
[22] Z. Anfar, et al., Microwave assisted green synthesis of Fe2O3/biochar for ultrasonic removal of nonsteroidal antiinflammatory pharmaceuticals, R. Soc. Chem. 10 (2020) 11371–11380.
[23] P.N Diagboya, et al., Clay-carbonaceous material composites: Towards a new class of functional adsorbents for water treatment, Surf. Interfaces 19 (2020) 100506.
[24] M. Arif, et al., Synthesis, characteristics and mechanistic insight into the clays and clay minerals-biochar surface interactions for contaminants removal-A review, J. Clean. Prod. 310 (2021) 127548.
[25] A. Maged, et al., Synergistic mechanisms for the superior sorptive removal of aquatic pollutants via functionalized biochar-clay composite, Bioresour. Technol 387 (2023) 129593.
[26] Y. Yao, et al., Characterization and environmental applications of clay–biochar composites, Chem. Eng. J. 242 (2014) 136–143.
[27] B.I. Olu-Owolabi, et al., Utilizing eco-friendly kaolinite-biochar composite adsorbent for removal of ivermectin in aqueous media, J. Environ. Manage 279 (2021) 111619.
[28] B. Zhang, et al., One-pot synthesis of MnFe2O4 functionalized magnetic biochar by the sol-gel pyrolysis method for diclofenac sodium removal, J. Clean. Prod. 381 (2022) 135210.
[29] P.N. Diagboya, et al., Comparative empirical evaluation of the aqueous adsorptive sequestration potential of low-cost feldspar-biochar composites for ivermectin, Colloids Surf. A: Physicochem. Eng. Asp. (2021) 127930.
[30] P.N. Diagboya, E.D. Dikio, Scavenging of aqueous toxic organic and inorganic cations using novel facile magneto-carbon black-clay composite adsorbent, J. Clean. Prod. 180 (2018) 71–80.
[31] B.I. Olu-Owolabi, et al., Empirical aspects of an emerging agricultural pesticide contaminant retention on two sub-Saharan soils, Gondwana Res. 105 (2022) 311–319.
[32] L.M. Madikizela, L. Chimuka, Synthesis, adsorption and selectivity studies of a polymer imprinted with naproxen, ibuprofen and diclofenac, J. Environ. Chem. Eng. 4 (4) (2016) 4029–4037.
[33] P.N. Diagboya, S.O. Akpotu, E. Osabohien, Ordered mesoporous silica to the rescue: A potential anti-contamination ally for pesticide capture in soil, Colloids Surf. A: Physicochem. Eng. Asp. 715 (2025) 136634.
[34] J. Junck, et al., Mechanistic interpretation of the sorption of terbuthylazine pesticide onto aged microplastics, Environ. Pollut. 345 (2024) 123502.

[35] P.R. Sera, et al., Potential of valourized Moringa oleifera seed waste modified with activated carbon for toxic metals decontamination in conventional water treatment, Bioresour. Technol. Rep. 16 (2022) 100881.
[36] R.P. Mohubedu, et al., Magnetic valorization of biomass and biochar of a typical plant nuisance for toxic metals contaminated water treatment, J. Clean. Prod. 209 (2019) 1016–1024.
[37] F. Güzel, et al., Performance of grape (Vitis vinifera L.) industrial processing solid waste–derived nanoporous carbon in copper(II) removal, Biomass Convers. Biorefinery 11 (4) (2020) 1363–1373.
[38] I. Villaescusa, et al., Removal of copper and nickel ions from aqueous solutions by grape stalks wastes, Water. Res 38 (4) (2004) 992–1002.
[39] S.O. Akpotu, et al., Designer composite of montmorillonite-reduced graphene oxide-PEG polymer for water treatment: enrofloxacin sequestration and cost analysis, Chem. Eng. J. 453 (1) (2023) 139771.
[40] B. Czech, et al., Engineered biochars from organic wastes for the adsorption of diclofenac, naproxen and triclosan from water systems, J. Clean. Prod. 288 (2021) 125686.
[41] E.B. AttahDaniel, et al., Adsorption investigation of a composite of metal-organic framework and polyethylene oxide hydrogel, Proc. Inst. Mech. Eng. N: J. Nanomater. Nanoeng. Nanosyst. (2023), https://doi.org/10.1177/23977914231195748(0), p. 23977914231195748.
[42] X. Feng, et al., Enhanced adsorption of naproxen from aquatic environments by β-cyclodextrin-immobilized reduced graphene oxide, Chem. Eng. J. 412 (2021) 128710.
[43] C.Y. Abasi, P.N.E. Diagboya, E.D. Dikio, Layered double hydroxide of cobalt-zinc-aluminium intercalated with carbonate ion: preparation and Pb(II) ion removal capacity, Int. J. Environ. Stud. 76 (2) (2018) 251–265.
[44] A.N. Ebelegi, et al., Covalently bonded polyamidoamine functionalized silica used as a Pb(II) scavenger from aqueous solution, J. Environ. Chem. Eng. 7 (4) (2019) 103214.
[45] V.M. Vulava, et al., Sorption, photodegradation, and chemical transformation of naproxen and ibuprofen in soils and water, Sci, Total, Environ. 565 (2016) 1063–1070.
[46] H.E. Reynel-Avila, et al., Assessment of naproxen adsorption on bone char in aqueous solutions using batch and fixed-bed processes, J. Mol. Liq. 209 (2015) 187–195.
[47] B.I. Olu-Owolabi, et al., Fractal-like concepts for evaluation of toxic metals adsorption efficiency of feldspar-biomass composites, J. Clean. Prod. 171 (2018) 884–891.
[48] C. Jung, et al., Competitive adsorption of selected non-steroidal anti-inflammatory drugs on activated biochars: Experimental and molecular modeling study, Chem. Eng. J. 264 (2015) 1–9.
[49] D. Shan, et al., Preparation of ultrafine magnetic biochar and activated carbon for pharmaceutical adsorption and subsequent degradation by ball milling, J. Hazard. Mater. 305 (2016) 156–163.
[50] D. Chen, et al., Activated biochar derived from pomelo peel as a high-capacity sorbent for removal of carbamazepine from aqueous solution, RSC Adv. 7 (87) (2017) 54969–54979.
[51] S. Jemutai-Kimosop, et al., Insights on adsorption of carbamazepine onto iron oxide modified diatomaceous earth: Kinetics, isotherms, thermodynamics, and mechanisms, Environ. Res 180 (2020) 108898.
[52] R. Guillossou, et al., Influence of dissolved organic matter on the removal of 12 organic micropollutants from wastewater effluent by powdered activated carbon adsorption, Water, Res 172 (2020) 115487.
[53] Y. Gao, M.A. Deshusses, Adsorption of clofibric acid and ketoprofen onto powdered activated carbon: effect of natural organic matter, Environ. Technol. 33 (15-16) (2011) 1719–1727.
[54] L. Lin, W. Jiang, P. Xu, Comparative study on pharmaceuticals adsorption in reclaimed water desalination concentrate using biochar: Impact of salts and organic matter, Sci, Total, Environ. 601-602 (2017) 857–864.
[55] H. Zhong, et al., Efficient adsorption removal of carbamazepine from water by dual-activator modified hydrochar, Sep. Purif. Technol. 353 (2025).